SHEAR BEHAVIOR AND BOND PERFORMANCE ALONG PC TENDONS IN PRESTRESSED REINFORCED CONCRETE INTERIOR BEAM-COLUMN SUBASSEMBLAGE UNDER BI-LATERAL LOAD REVERSALS

Tajima Yuji[1], Kitayama Kazuhiro[2] and Yajima Ryuto[3]

[1] *Graduate School of Engineering ,Tokyo Metropolitan University, M. Eng, Japan*
[2] *Associate Professor, Graduate School of Engineering, Tokyo Metropolitan University, Dr. Eng, Japan*
[2] *Graduate School of l Engineering, Tokyo Metropolitan University, Japan*
Email: tajima-yuji@ed.tmu.ac.jp

ABSTRACT :

It is very important to clarify joint-panel shear failure mechanism of prestressed reinforced concrete (PRC) structures in which both PC tendons and longitudinal reinforcing bars are arranged. Therefore, bi-lateral load reversal tests of PRC three-dimensional and plane interior beam-column subassemblage specimens fabricated by post-tensioning method were carried out to investigate joint-panel shear behavior and bond performance along a PC tendon-sheath tube system. After column flexural yielding occurred for the three-dimensional specimen with coarse spacing of ribs along sheath tube surface a joint panel failed eventually in shear. As for the three-dimensional specimen with close spacing of ribs along sheath tube surface, the column failed in flexure without decay of story shear capacity.

KEYWORDS: Prestressed Reinforced Concrete, Three-Dimensional Interior Beam-Column Subassemblage, Joint-Panel Shear Behavior, Sheath Tube Bond

1. OBJECTIVES

It is very important to clarify joint-panel shear failure mechanism of prestressed reinforced concrete (called as PRC) structures in which both PC tendons and longitudinal reinforcing bars are arranged. However, shear failure mechanism of interior beam-column joint-panels in PRC structures is not resolved yet under bi-lateral loading. Moreover, the bond condition along a combined system of a PC tendon and a sheath tube filled with grout (called as a PC tendon-sheath system) is very complex. Past studies indicate that good bond along beam longitudinal bars passing through a reinforced concrete (called as RC) joint-panel enhances joint-panel shear strength [1]. In the same manner, it is probable that joint-panel shear strength in PRC structures is influenced by the bond along the PC tendon-sheath system. Therefore, bi-lateral load reversal tests of PRC three-dimensional and plane interior beam-column subassemblage specimens fabricated by post-tensioning method were carried out to investigate joint-panel shear behavior and bond performance along the PC tendon-sheath system.

2. TEST PROGRAM

2.1. Specimens

Properties of specimens are summarized in Table 1. Material properties of concrete, grout, and steel are listed in Tables 2, and 3, respectively. Section dimensions and reinforcement details are shown in Fig.1. Four specimens were fabricated with two-fifth scale and called JP-1, JP-2, JD-3 and JD-4. Plane beam-column joint specimens were JP-1 and JP-2. Three-dimensional interior joint specimen JD-3 or JD-4 was accompanied by a plane specimen JP-1 or JP-2, respectively, with common bar arrangement and section dimensions. The surface shapes of a used sheath tube are shown in Fig.2. Rib spacing along the surface of a sheath tube which contains PC tendons and passes through beams and a joint-panel was varied, i.e., coarse and close spacing of the ribs. Sheath tubes for specimens JP-1 and JD-3 had coarse spacing of the ribs (called as #1040) and those for specimens JP-2 and JD-4 had close spacing of the ribs (called as #3040). The column section was square with

350mm depth and width. The depth and width of the beam section were 400mm and 250mm, respectively. One set of 2-D10 was arranged in a beam-column joint panel as lateral reinforcement. The length from a center of the column to the support of a beam end was 1600mm. The height from a center of the beam to the loading point on the top of the column or to the bottom support was 1415mm, respectively. The shear span ratio was 3.5 for the column and 3.7 for the beam.

All specimens were designed to fail in joint shear, using 22mm-diameter deformed bars as a post-tensioning steel. Concrete compressive strength was 77MPa. Grout compressive strength was 65MPa. The post-tensioning force equivalent to the stress 0.6 times the yield strength of the PC tendon was provided initially. Bond along post-tensioning steel bars was provided by injecting grout mortar into a sheath tube.

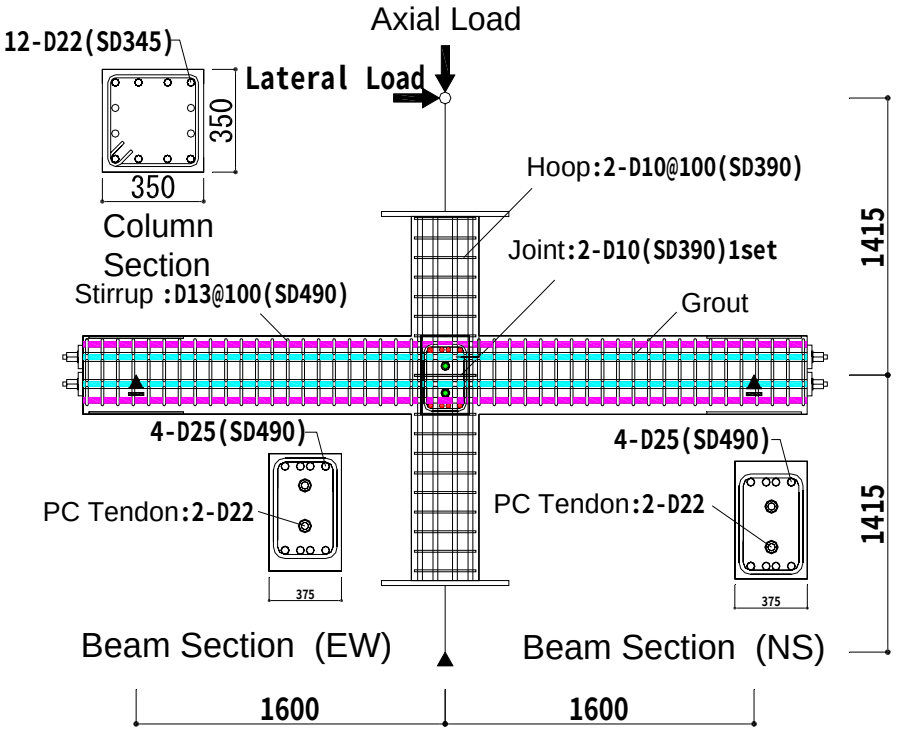

Fig.1 Section dimensions and reinforcement details

Table1. Properties of specimens

Specimen	JP-1	JP-2	JD-3	JD-4
Shape	Plane		Three-dimensional	
Beam longitudinal bars	4-D25			
Post-tensioning beam bars	2-D22			
Beam stirrup (Pw,%)	**D13@80(1.27%)**			
Column longitudinal bars	12-D22			
Column hoop (Pw,%)	**2-D10@100(0.41%)**			
Column axial load	930 kN			
Joint lateral hoop	2-D10 1set			
λ^{*1}	0.26			

*1:λ=(Ultimate moment shared by PC tendon)/(Ultimate moment)

Photo.1. Loading apparatus

Table2. Material properties of concrete and grout

Specimen		JP-1	JP-2	JD-3	JD-4
Concrete	Compressive strength	77.2MPa			
	Secant modulus*1	40.7GPa			
	Strain at compressive strength	0.29%			
	Tensile strength	4.29MPa			
Grout	Compressive strength	65.3MPa			
	Secant modulus*1	22.2GPa			
	Strain at compressive strength	0.51%			
	Tensile strength	2.66MPa			

*1:Secant modulus at one-quarter of the compressive strength

Table3. Material properties of steel bars

Diameter	Yield strength MPa	Nominal Young's modulus GPa	Yield strain %
D22(PC tendon)*1	1042	200	0.73
D25	550	193	0.29
D22	387	185	0.21
D10	444	199	0.22

*1:Yield strength and strain were determined by 0.2% offset method.

2.2. Loading Method and Instrumentation

A loading apparatus is shown in Fig.3 and Photo.1. The beam ends were supported by horizontal rollers, while the bottom of the column was supported by a universal joint. The reversed bi-lateral horizontal loads and the constant axial load in compression (an axial load ratio of 0.10) were applied at the top of the column through a tri-directional joint by three oil jacks. All Specimens were controlled by a story drift angle for one loading cycle of 0.25 %, two cycles of 0.5 %, 1 %, 1.5% and 2 % respectively, one cycle of 3 %, two cycles of 4 % and one-way loading to 5 %. Loading paths at the top of the column under bi-lateral load reversals are shown in Fig.4; when an identical story drift angle was given in two loading cycles, solid line was traced for the first loading cycle and then dashed line for the second loading cycle. For all bi-lateral loading cycles, at first the lateral force in the east-west direction was applied and then the lateral force in the north-south direction was applied while keeping the story drift in the east-west direction constant. Lateral forces, column axial load and beam shear forces were measured by load-cells. Story drift, beam and column deflections, and local displacement of a joint panel were measured by displacement transducers. Strains of prestressing steel bars, beam bars, column bars and joint lateral reinforcement were measured by strain gauges. Concrete normal strain at a beam end adjacent to a column face was measured by strain gauges attached on concrete surface.

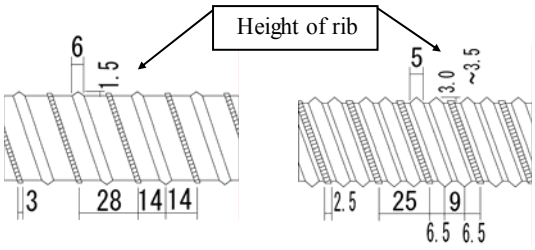

(a) # 1040 (b) # 3040

Fig.2 Shape of sheath tube

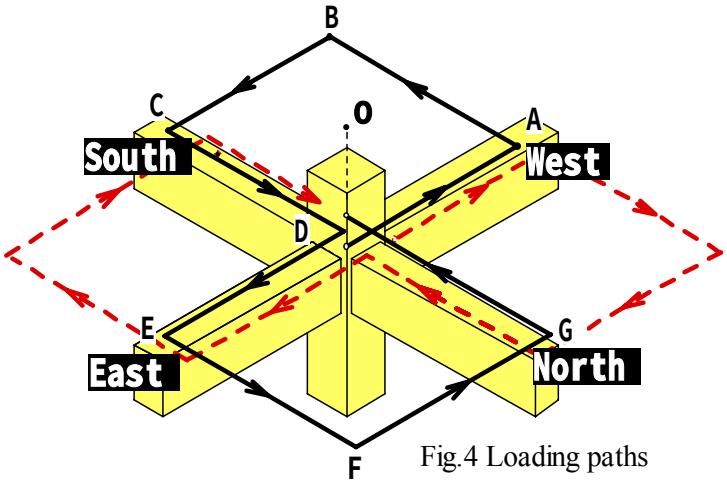

Fig.4 Loading paths

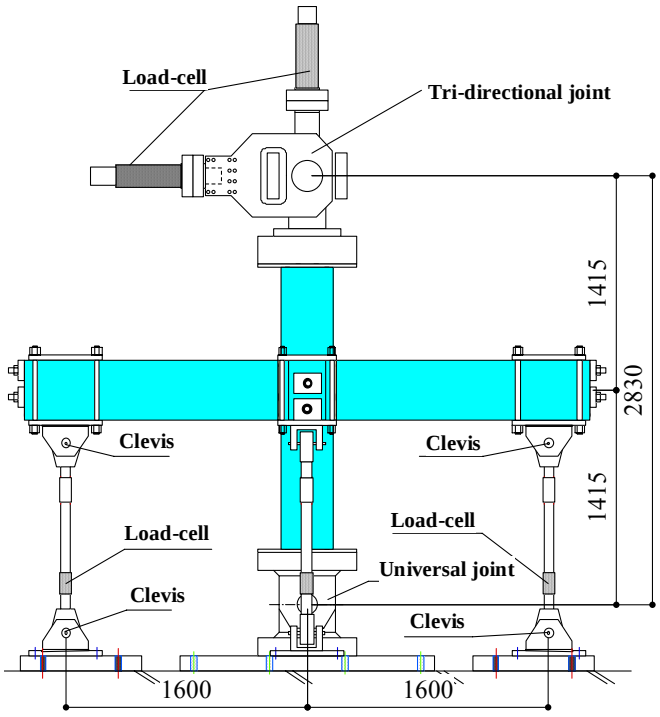

Fig.3 Loading apparatus

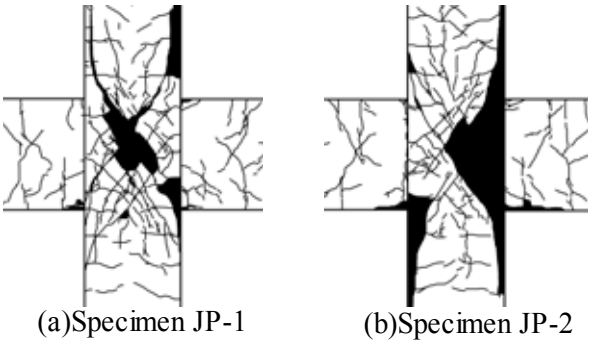

(a)Specimen JP-1 (b)Specimen JP-2

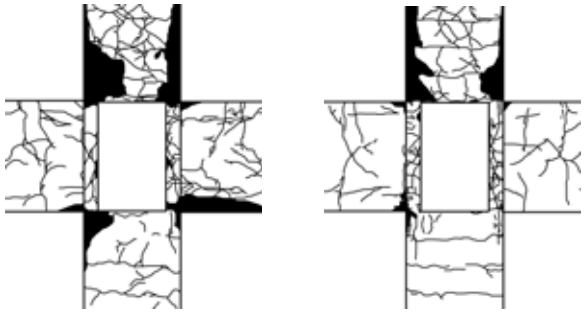

(c)Specimen JD-3 (d)Specimen JD-4

Fig.5 Crack Patterns

3. TEST RESULTS AND DISCUSSIONS

3.1. General Observations and Story Drift Contribution

Crack patterns at a story drift angle of 4 % are shown in Fig.5. Many diagonal shear cracks occurred in the beam-column joint region for all specimens. For three-dimensional specimens JD-3 and JD-4, cover concrete at corners in the joint region spalled off and concrete in the column and the beam hinge regions adjacent to the joint region crushed and spalled off remarkably due to bi-lateral cyclic loading. Post-tensioning beam bars and beam bars did not yield for all specimens. Column bars did not yield for plane specimens. On the other hand, for three-dimensional specimens JD-3 and JD-4, column bars yielded at a story drift angle of 1.5 %.

The contribution of deformation of beams, a column and a joint panel to the story drift was calculated and shown in Fig.6. The horizontal axis represents the measured story drift. Sum of each component for plane beam-column joint specimens did not always correspond with the directly measured story drift, including a little tolerance due to using the measured displacement of each component. The contribution of a joint panel deformation for three-dimensional specimens was calculated as the total deflection less the contribution from the beam and column deflections. The beam-column joint panel deformation increased for plane specimens and specimen JD-3 after the peak story shear force. On the other hand, the ratio of deformation of beams, a column and a joint panel to the story drift was almost constant for three-dimensional specimen JD-4 with a sheath tube of #3040.

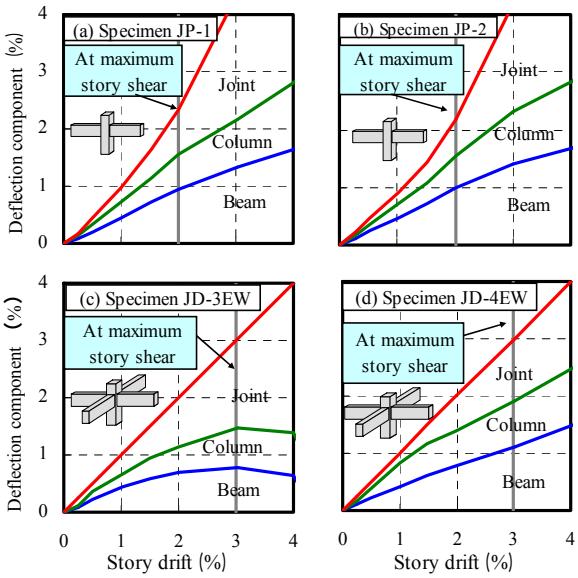

Fig.6 Deflection component of story drift

3.2. Story Shear – Drift Relations

The story shear force - story drift relations are shown in Fig.7. Peak story shear forces obtained by the tests are summarized in Table 4. The story shear force was computed from moment equilibrium between measured beam shear forces and the horizontal force at the loading point on the top of the column. Yielding point of column longitudinal bars and peak point of the story shear force are shown by squares and solid circles in Fig.7, respectively. The peak story shear

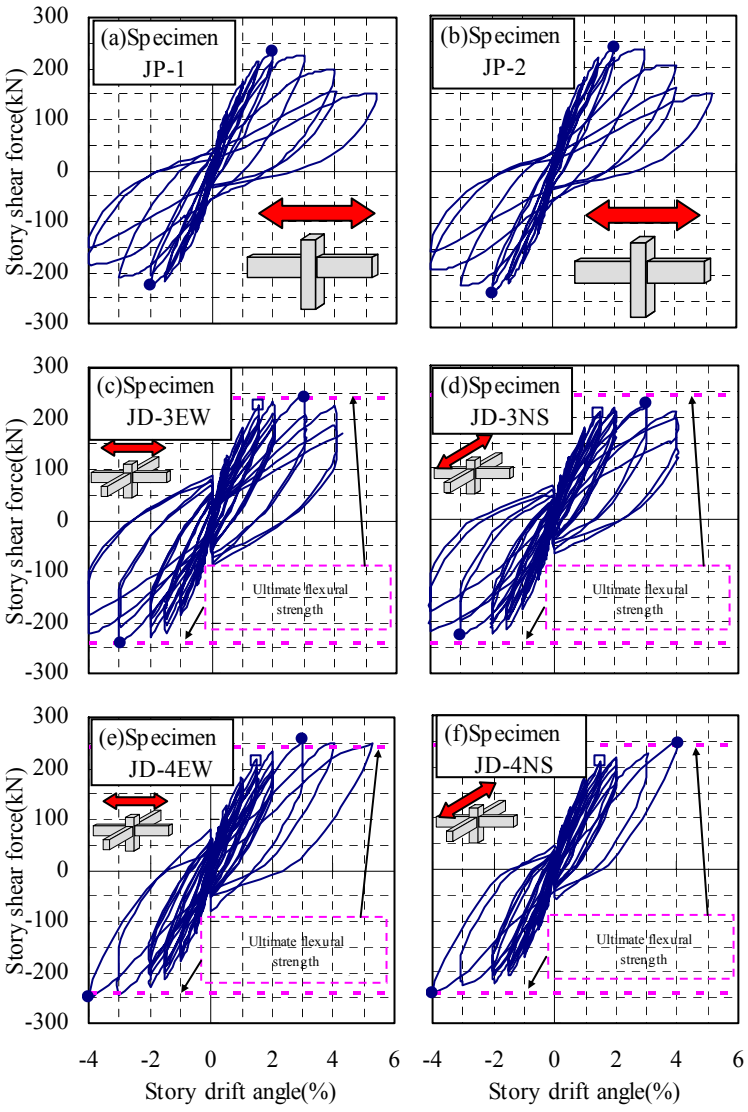

Fig.7 Story shear force-Story drift angle relations

force was attained at a story drift angle of 2 % and 3% for plane specimens and three-dimensional specimens, respectively. The peak story shear forces and envelope curves were almost equal between plane interior beam-column joint specimens JP-1 and JP-2.

Table.4 Peak story shear Unit in kN

Specimen	JP-1	JP-2	JD-3		JD-4	
Loading direction	EW	EW	EW	NS	EW	NS
Positive loading	234	238	250	225	255	246
Negative loading	227	235	242	224	250	241

Ultimate flexural strength of the column calculated according to seismic design provisions by Architectural Institute of Japan [2] is shown by a dotted line. Story shear forces for three-dimensional specimens JD-3 and JD-4 reached the predicted ultimate strength of the column. For three-dimensional specimen JD-3, the peak story shear force in the east-west direction was 6.8 percent as large as that for plane specimen JP-1 with the same dimensions. This indicates that the interior beam-column joint strength was enhanced by two transverse beams framing into a joint panel compared with that of a plane beam-column joint. The story shear force decreased after the peak because of severe damage of the corner concrete in a joint region for three-dimensional specimen JD-3 with a sheath tube of #1040. On the other hand the story shear force kept about 250(kN) from a story drift angle of 3% to 5% for three-dimensional specimen JD-4 with a sheath tube of #3040.

3.3. Failure Mode

The beam-column joint panel for three-dimensional specimen JD-3 eventually failed in shear after yielding of column bars. The column hinge region adjacent to a joint panel for three-dimensional specimen JD-4 failed in flexure because of yielding of column bars. Joint shear failure occurred for both plane specimens JP-1 and JP-2.

3.4. Joint Shear Force

Envelope curves of the relations between joint shear stress and a joint shear distortion angle are shown in Fig.9 for plane specimens JP-1 and JP-2. Joint shear lower and mean strengths of R/C beam-column joints calculated according to seismic design provisions by Architectural Institute of Japan [3] are also shown by dotted and broken line, respectively. The joint shear force denoted as V_{jh} was computed from beam bar and post-tensioning beam bar stresses, which were obtained from measured strain, by Equations (1) or (2) described in following paragraphs 1) and 2) using the notations shown in Fig.8. Fig.8 shows a stress condition of plane specimen JP-1 around a beam-column joint at a story drift angle of 2%. It is important whether both concrete compressive stress distributions on opposed beam critical sections overlap in the central region across the joint panel as shown in Fig.8. When the distance from the extreme compression fiber to the neutral axis (the depth of the concrete compressive stress distribution) is greater than the half of the beam depth, the maximum joint shear force can be obtained mathematically in the horizontal section on the beam center axis. Therefore the joint shear force is computed as Equation (2).

1) when the depth of the compressive stress distribution on the beam critical section is less than or equal to the half of the beam depth;

$$V_{jh} = T_{s1} + T_{p1} + T_{s2} + T_{p2} - V_c \quad (1)$$

2) when the depth of the compressive stress on the beam critical section is greater than the half of the beam depth;

$$Vjh = T_{s1} + T_{p1} - \alpha'_1 \bullet C_{c1} + \alpha'_2 \bullet C_{c2} - T'_{s2} - T'_{p2} - V_c \quad (2)$$

$$C_{c1} = T_{s1} + T_{p1} + T'_{p1} + T'_{s1} \quad (3)$$

$$C_{c2} = T_{s2} + T_{p2} + T'_{p2} + T'_{s2} \quad (4)$$

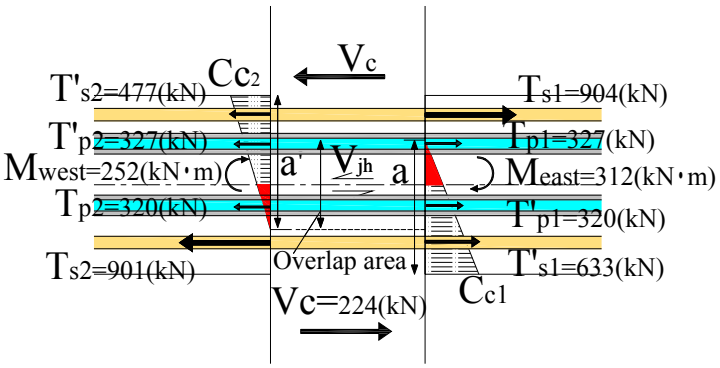

Fig.8 Stress acting on joint panel
(Specimen JP-1 at story drift angle of 2%)

$$\alpha_1 = 1 - \alpha_2 \quad (5)$$

$$\alpha_1' = 1 - \alpha_2' \quad (6)$$

$$\alpha_2 = (a - D/2)^2 / a^2 \quad (7)$$

$$\alpha_2' = (a' - D/2)^2 / a'^2 \quad (8)$$

where T_{p1} and T'_{p2} are tensile forces of the top post-tensioning beam bar, T_{s1} and T'_{s2} are tensile forces of the top beam bar, T_{p2} and T'_{p1} are tensile forces of the bottom post-tensioning beam bar, T'_{s1} and T_{s2} are tensile forces of the bottom beam bar, a and a' are the depth of the compressive stress distribution, and V_c is story shear force. The shape of the concrete compressive stress distribution was regarded as triangular on the basis of measured concrete strain by attached gauges on the beam surface at the location of 50mm apart from the beam critical section.

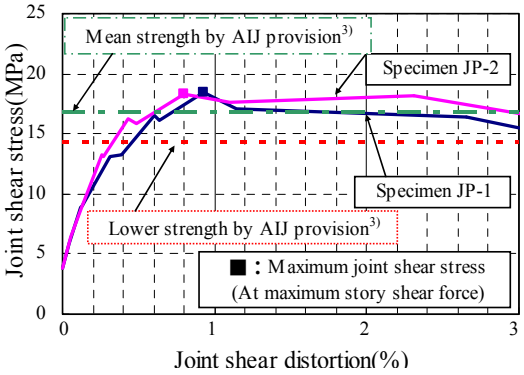

Fig.9 Joint shear stress-joint shear distortion angle relations

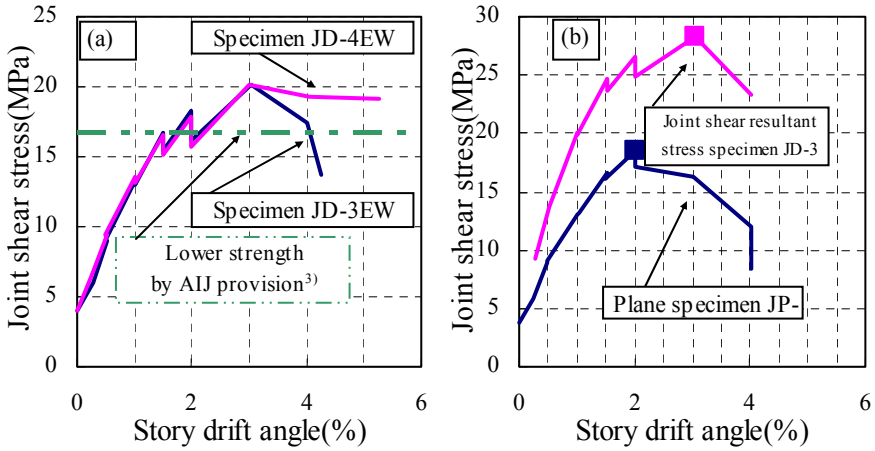

Fig.10 Joint shear stress-story drift angle relations

The joint shear force reached the peak at a joint shear distortion of about 0.93%, corresponding to a story drift angle of 2%, and then decreased as well as story shear force for plane specimens. The joint shear strengths for plane interior beam-column joint specimens were larger than predicted mean strength for R/C beam-column joints according to the AIJ provisions [3]. Joint shear stress-distortion relations for specimens JP-1 and JP-2 were little different until the peak shear stress.

Envelope curves of the relations between joint shear stress in the east direction and a story drift angle are shown in Fig.10 (a) for three-dimensional specimens JD-3 and JD-4. Joint shear lower strength of R/C beam-column joints calculated according to seismic design provisions by Architectural Institute of Japan [3] is also shown by a broken line. The joint shear strengths for three-dimensional interior beam-column joint specimens were larger than predicted lower strength for R/C beam-column joints according to the AIJ provisions [3]. Joint shear stress-distortion relations for specimens JD-3 and JD-4 were almost same until the peak. After the peak, joint shear stress for specimen JD-3 decreased remarkably due to shear failure in a joint panel, and that for specimen JD-4, which failed in column flexure decreased slightly. The beam-column joint shear strength for three-dimensional specimen JD-4 using a sheath tube of #3040 was, therefore, larger than that for specimen JD-3 using a sheath tube of #1040. The resultant shear stress in a joint panel for three-dimensional specimen JD-3 under bi-lateral loading is shown in Fig.10 (b), compared with the joint shear stress for plane specimen JP-1 under uni-lateral loading. The resultant joint shear strength for three-dimensional specimen JD-3 under bi-lateral loading was enhanced to 1.52 times that for plane specimen JP-1.

3.5. Bond along Prestressing Beam Bar in Beam-Column joint

Strain distribution along a prestressing beam bar for plane specimen JP-1 is shown in Fig.11 at each peak story drift angle. Strain gauges along prestressing beam bars within a joint panel were attached to two points denoted as G1 and G2 as illustrated in Fig.11. Prestressing bar strain at the point G2 was larger than that at the point G1

at a story drift angle of 0.25%. On the contrary, prestressing bar strain at the point G1 exceeded that at the point G2 after the occurrence of joint shear cracks at a story drift angle of 0.5%. This tendency was observed for all specimens. This was caused by local tensile strain due to a joint shear crack near the location of the prestressing bar strain gauge. The local bond stress along a prestressing beam bar was computed by the difference in prestressing beam bar forces between the critical section in compression side and the point G1 (the area enclosed by dotted line in Fig.11).

Envelope curves of the relations between a local bond stress along a prestressing beam bar and a story drift angle are shown in Fig.12. Maximum bond stresses are shown by solid squares in Fig.12. The average of maximum local bond stresses along a prestressing beam bar was 5.1MPa. Maximum local bond stresses along a prestressing beam bar were little different among all specimens because bond deterioration occurred along the interface between the PC tendon and grout mortar.

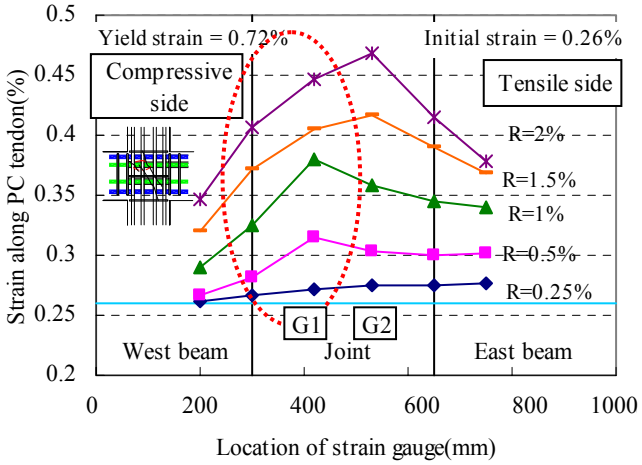

Fig.11 Strain distribution along PC tendon

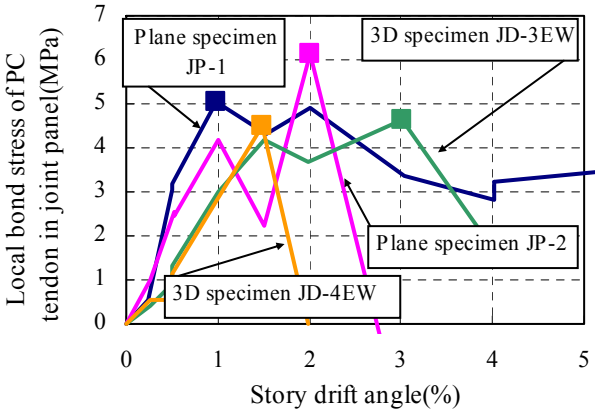

Fig.12 Local bond stress of PC tendon in joint panel-Story drift angle relations

3.6. Beam Bar Bond in Beam-Column joint

Envelope curves of the relations between beam bar bond stress in the beam-column joint and a beam bar slip at a center of a joint panel are shown in Fig.13 for plane specimens JP-1 and JP-2. The local beam bar bond stress in a joint panel was computed by the difference between beam bar forces in the middle one-third region of a joint panel with a length of 110mm. Relative displacement between a beam bar and concrete at a center of a joint panel was regarded as a beam bar slip, which was measured by the transducer mounted as shown in Fig.14. The beam bar bond stresses at maximum story shear are shown by a diamond in Fig.13. Beam bar bond stresses for specimens JP-1 and JP-2 were little different until maximum story shear. After maximum story shear, beam bar bond stress for specimen JP-1 using a sheath tube of #1040 decreased, but that for specimen JP-2 using a sheath tube of #3040 increased until a beam bar slip of 0.4mm. The peak beam bar bond stress in a joint panel for plane specimen JP-2 using a sheath tube of #3040 was enhanced to 1.57 times that for plane specimen JP-1 using a sheath tube of #1040. This indicates that damage of concrete in a joint panel for specimen JP-2 using a sheath tube of #3040 was less than that for specimen JP-1 using a sheath tube of #1040.

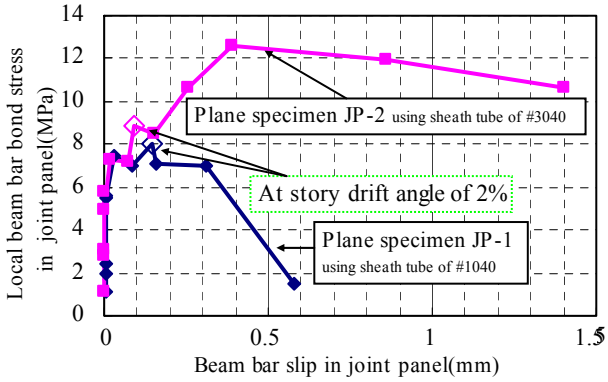

Fig.13 Local beam bar bond stress in joint panel-Beam bar slip relations

3.7. Deformation in Joint Panel

The lateral and vertical displacements in a joint panel are shown in Fig.15 by a solid line for plane specimen JP-1 and a dotted line for plane specimen

JP-2. The joint panel for both specimens expanded to the lateral direction. At a story drift angle of 4%, lateral displacement for plane specimen JP-1 using a sheath tube of #1040 was 1.2 times as large as that for plane specimen JP-2 using a sheath tube of #3040. To use a sheath tube with close rib spacing on the surface, which may improve the bond condition to surrounding concrete, prevented concrete in a joint panel from expanding to the lateral direction after maximum story shear.

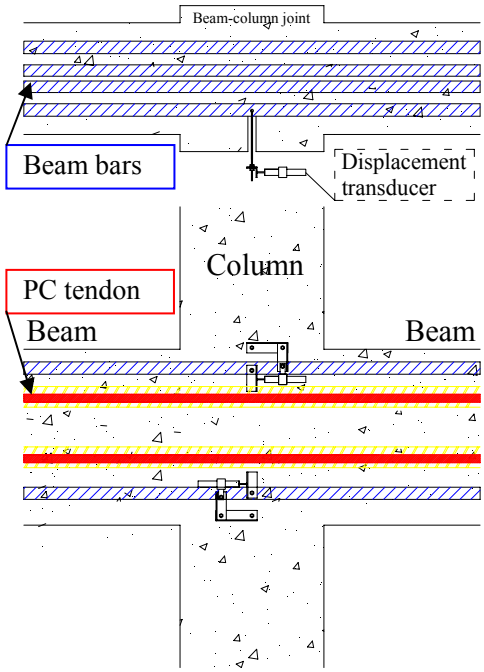

Fig.14 Measuring method for beam bar slip in joint panel

4. CONCLUSION

(1) A joint panel failed in shear for plane specimens. Shear strength of a beam-column joint panel in three-dimensional specimens was enhanced by confining effect due to transverse beams on joint-panel core concrete. After the three-dimensional specimen with coarse spacing of ribs along sheath tube surface resulted in column flexural yielding, finally it failed in joint-panel shear. As for the three-dimensional specimen with close spacing of ribs along sheath tube surface, the column failed in flexure without decay of story shear capacity.

(2) Joint shear stress for specimen JD-3 decreased remarkably due to shear failure in a joint panel. That for specimen JD-4, not failing in joint shear, decreased slightly after the peak stress. The beam-column joint shear strength for three-dimensional specimen JD-4 using a sheath tube of #3040 was, therefore, larger than that for specimen JD-3 using a sheath tube of #1040.

(3) Maximum local bond stresses along a prestressing beam bar were little different among all specimens because bond deterioration occurred along the interface between the PC tendon and grout mortar.

(4)To use a sheath tube with close rib spacing on the surface, which may improve the bond condition to surrounding concrete, prevented concrete in a joint panel from expanding to the lateral direction after maximum story shear.

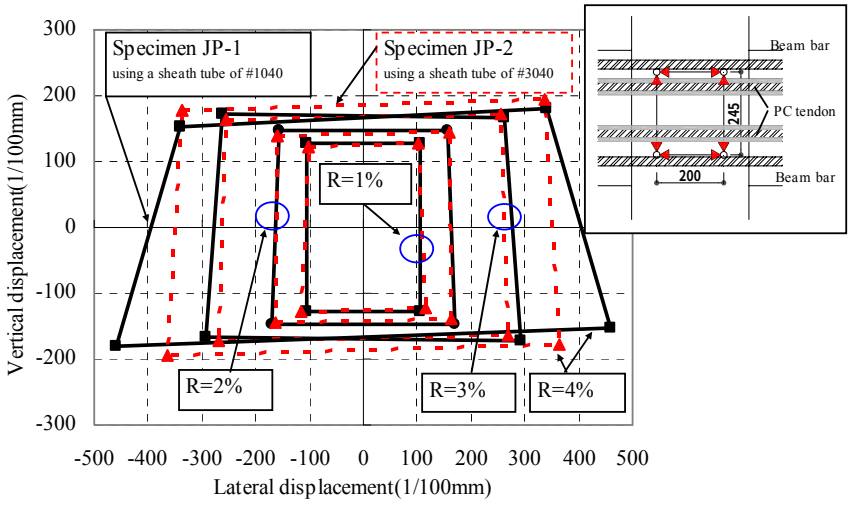

Fig.15 Vertical displacement-lateral displacement relations in joint panel

REFERENCES

1. Kitayama K., Tajima Y., Okuda M., Kishida S. *Influences of Beam and Column Bar Bond on Failure Mechanism in Reinforced Concrete Interior Beam-Column Joints*, *Transactions of The Japan Concrete Institute*, 2000, vol.22,pp.433-440.
2. Architectural Institute of Japan. *Data for Ultimate Strength Design of Reinforced Concrete Structures*, 1987.
3. Architectural Institute of Japan. *Design Guideline for Earthquake Resistant Reinforced Concrete Buildings Based on Inelastic Displacement Concept*, 1999.